Geoffroy Hautier

View Online   Export Citation

ARTICLES YOU MAY BE INTERESTED IN

Prediction of New Battery Materials Based on *Ab initio* Computations

Geoffroy Hautier[1,a)]

[1]*Institute of Condensed Matter and Nanosciences (IMCN), Université catholique de Louvain, chemin des étoiles 8, 1348 Louvain-la-Neuve, Belgium*

[a)]Corresponding author: geoffroy.hautier@uclouvain.be

Abstract. First principles or *ab initio* computations are revolutionizing the materials design process. The advent of high-throughput computational screening is especially disruptive. By computing properties for thousands of materials, researchers can now target the chemistries and compounds of greatest interest. In this short review paper, we present an overview of the status of computational Li-ion battery electrode design. We focus especially on high-throughput search and on cathode materials. We review briefly the properties assessable through first principles computations and present results of high-throughput computational screening approaches. We also highlight the importance of using large computational databases to perform data mining studies and explore the correlations, chemical trends and limits in cathode materials properties.

INTRODUCTION

Li-ion batteries have become the leading technology in energy storage and enabled the small electronic revolution leading to the widespread use of mobile phones and laptops. However, many challenges lie ahead to transfer this technology to new applications especially in transport. Improvements in the intrinsic materials properties (*e.g.*, energy density and rate capability) of the battery components (*i.e.*, cathode, anode and electrolyte) are intensively sought for [1, 2, 3, 4].

Most battery properties are nowadays assessable through *ab initio* or first principles computations which aim at solving the fundamental equations of quantum mechanics to model and even predict materials properties. *Ab initio* computations are revolutionizing materials science and the field of Li-ion battery is no exception. First principles computations are readily used to understand, identify and design new materials for Li-ion battery electrodes. The theoretical techniques have reached such maturity that they have recently started to be used to perform high-throughput computational search of materials. By computing properties on large databases of thousands of potential electrode materials, researchers can identify the most promising compounds to be targeted by follow-up experimental work.

This short review paper will present first the different batteries properties available through first principles computations. It will then describe how high-throughput computing can help the discovery of novel electrode materials providing several examples of studies combining theoretical prediction and experimental verification. The emphasis will also be on the use of the large materials properties databases to perform data mining studies aimed at identifying correlations and trends in materials properties. Our ambition is not to perform an exhaustive survey of the large body of work using first principles computations in lithium-ion batteries. We propose instead a personal perspective on some of the recent developments especially in high-throughput computational prediction of battery materials. We refer the interested reader to other review papers for more in-depth reviews on first-principle computations for Li-ion batteries [5, 6, 7, 8].
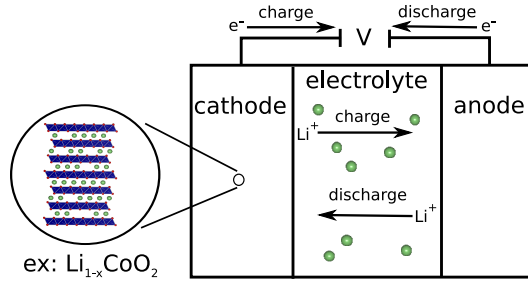
FIGURE 1. Schema of a lithium-ion battery. A zoom of the crystal structure of a typical cathode material ($LiCoO_2$) on the atomic scale is shown. Oxygen is in red. Cobalt sits in blue CoO_6 octahedra and lithium is in green.

AB INITIO COMPUTATIONS AND BATTERY PROPERTIES

Lithium-Ion Batteries

A battery is an electrochemical device used to store energy [9]. Two types of batteries exist: primary batteries, which can only be discharged once, and secondary (or rechargeable) batteries which can be charged and discharged multiple times. Our focus will be on rechargeable batteries.

A battery consists of two electrode materials (the cathode and the anode) separated by an electrolyte (see Fig. 1). For Li-ion technology, the electrolyte is a poor electron conductor but a good lithium ion conductor. The cathode is typically a transition metal oxide (*e.g.*, $LiCoO_2$) and the anode is metallic lithium in laboratory settings or graphitic carbon in commercial cells. During charge, an electrical potential difference is applied between the cathode and anode. The lithium ions flow then through the electrolyte from the cathode to the anode. The $LiCoO_2$ cathode is depleted from lithium and the graphitic carbon is filled with lithium according to the two chemical reactions:

$$LiCoO_2 \rightarrow x\,Li + Li_{1-x}CoO_2 \tag{1}$$

$$x\,Li + C_y \rightarrow Li_xC_y \tag{2}$$

During discharge, the opposite reactions occur. The difference between the high lithium chemical potential at the anode and the low chemical potential of lithium in the cathode makes the lithium ions flow from the anode to the cathode. The lithium intercalates back into the $LiCoO_2$ cathode and the graphitic carbon anode looses lithium. An electrical potential is then available between the two electrodes and the following reactions occur:

$$Li_{1-x}CoO_2 + x\,Li \rightarrow LiCoO_2 \tag{3}$$

$$Li_xC_y \rightarrow C_y + x\,Li \tag{4}$$

Please note that during these charge and discharge processes, the transition metal present in the oxide cathode is oxidized/reduced between Co^{3+} and Co^{4+}.

In this work, we will only consider *insertion* batteries. Insertion materials intercalate or deintercalate lithium ions in a fixed structural framework. For instance, the layered crystal structure of $LiCoO_2$ is conserved while lithium ions are removed and replaced by vacancies. When the structural framework is not conserved, one speaks of *conversion* electrodes. Insertion batteries tend to be more reversible and exhibit less hysteresis between charge and discharge [10].

Some of the general key requirements for a lithium-ion insertion battery cathode material have been listed [1]. Depending on the application, the weight attributed to those requirements can vary.

- Considerable amounts of energy can be stored per unit of mass (Wh/kg) or volume (Wh/l). This requires a high *capacity* (*i.e.*, the amount of charge that can be inserted between charge and discharge) per unit mass (mAh/g) or volume (mAh/cm^3) and a high *voltage*. The energy density is the product of the capacity and the voltage. Typical energy densities for cathode materials are from 600 Wh/kg ($LiFePO_4$) to 800 Wh/kg (layered nickel cobalt manganese oxides).

- The material needs to be *cyclable* (*i.e.*, be able to be charged and discharged many times with minimal capacity fade).
- The voltage should not be too high. While a high voltage is usually sought to maximize the energy density, current commercial electrolytes decompose around a voltage of 4.5 V (with reference to lithium metal anode).
- Lithium needs to be able to diffuse fast enough in the bulk material. This is required for high-rate charge and discharge (*i.e.*, high power density).
- The material needs to be a good electronic conductor. Poor conductors can be used (*e.g.*, phosphates) but large amounts of inactive conductive additives such as carbon black are required then to ensure good electrical contact in the cathode powder.
- The material in the discharged state needs to be stable enough versus oxygen evolution to minimize safety hazard.
- The material needs to be produced at a reasonable cost.

Ab Initio Computed Properties

Ab initio computations rely on solving the fundamental equations of quantum physics to compute materials properties. This requires to solve the Schrödinger equation which is a many-body problem typically very challenging to tackle for most molecules and solids. To model realistic systems, computational materials scientists have to rely on powerful approximations such as density functional theory (DFT) [11, 12].

Some of the key properties mentioned in the previous section are controlled by intrinsic properties of the cathode materials. *Ab initio* computations have been used extensively to understand and predict those properties [5, 6, 7, 8].

Through a thermodynamical analysis, the average equilibrium voltage ($< V >$) of a cathode can be related to the difference in the Gibbs free energy between its charged state (delithiated phase) and discharged state (lithiated phase) [13]. If $Li_{x_1}X$ and $Li_{x_2}X$ are respectively the lithiated and delithiated states, the average voltage between these two lithiation states is

$$< V >= \frac{-[G(Li_{x_2}X) - G(Li_{x_1}X) - (x_2 - x_1)G(Li)]}{(x_2 - x_1)F}, \tag{5}$$

where $G(Li)$ is the Gibbs free energy of the lithium metal anode and F the Faraday constant.

Because the contributions of entropy and volume effects to the Gibbs free energy difference are typically small in solids, one may approximate the voltage using energy differences computed at zero temperature and pressure. Such an energy computation can be performed very easily by DFT. The average voltage is then

$$< V >\approx \frac{-[E(Li_{x_2}X) - E(Li_{x_1}X) - (x_2 - x_1)E(Li)]}{(x_2 - x_1)F}. \tag{6}$$

However, as cathode materials contain very often transition metals with partially occupied *d*-shells, traditional DFT (*e.g.*, in the generalized gradient approximation, GGA) can be inaccurate. More advanced techniques such as DFT+U [14] or hybrid functionals [15, 16] are needed to accurately predict voltages. Fig. 2 demonstrates the good agreement between voltages computed using GGA+U or the HSE hybrid functionals and the experimental voltages for a variety of cathode materials. In average the computations deviate from experiment by only a few hundred mV. The HSE method has the advantage over GGA+U that it does not rely on a fitted parameter for each element. HSE computations are however computationally more expensive (in average 40 times more expensive than GGA+U). One of the first uses of first principles computations in the field of Li-ion batteries to perform materials design was the pioneering work from Ceder *et al.*, which computationally predicts an increase in $LiCoO_2$ voltage when alloyed with aluminum [17].

Safety is one of the key considerations in the design of a lithium-ion battery cathode. Charged cathodes can be a safety hazard. A typical runaway reaction in a lithium battery starts by an overheating event (*e.g.*, caused by an internal or external short), which causes the charged cathode to release oxygen. The released oxygen can potentially combust the flammable organic electrolyte and ultimately lead to fire. The safety of a cathode material can be assessed by computing phase diagrams from energies computed within DFT. More specifically, the temperature of oxygen release can be evaluated and used as an indicator of thermal stability. This methodology has been successfully used to compare the safety of delithiated $LiMnPO_4$ and delithiated $LiFePO_4$ [18]. Figure 3 presents a comparison of computed oxygen release temperature for $MnPO_4$ and $FePO_4$ indicating the lower thermal stability for the manganese phase.
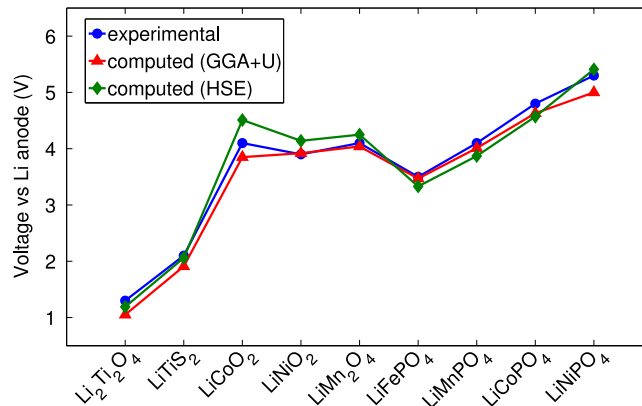
FIGURE 2. Comparison between experimental and computed (using GGA+U or HSE) voltages. As titanium does not require a U value to reproduce accurate energies, no U value was used for $Li_2Ti_2O_4$ and $LiTiS_2$. The data is from Chevrier *et al.* [16].

For a battery material to charge and discharge at a high enough rate (*i.e.*, to provide good power density), the lithium ions need to be able to diffuse fast enough in the material. Modeling diffusion in cathode materials involves the computations of energy barriers and the study of the vacancy and lithium ordering during discharge [19, 20]. A simpler but often sufficient approach is to focus only on the energy barriers. Small enough energy barriers to the lithium diffusion is a necessary requirement for fast diffusion. As a rule of thumb, the lowest lithium migration barrier needs to be lower than 500 meV − 600 meV for any battery material to be a good enough diffuser [21]. Migration barriers can be computed in the Nudge Elastic Band (NEB) framework with DFT computations. This approach has been used to predict that $LiFePO_4$ is an extremely fast one-dimensional diffuser with an activation barrier around 200 meV [22]. Materials design can be driven by DFT diffusion computations as shown by the crystal structure engineering performed by Kang *et al.* to improve the rate capability of layered $Li(Ni_{0.5}Mn_{0.5})O_2$ [23]. First principles diffusion studies involving kinetic monte-carlo modeling recently identified a percolation effect in Li-excess, rock-salt cathodes [24, 25]. Another recent development in the computational study of electrodes kinetics is the use of *ab initio* molecular dynamics simulation to assess Li diffusion activation barriers [26, 27, 28, 29, 30].

As well as fast lithium transport, fast electron transport is important for high rates in electrode materials. Cathode materials are often polaronic conductors. The limiting factor for the electronic conductivity is then the mobility of the small polaron. The polaron migration barrier can be computed *ab initio* as shown for $LiFePO_4$ [31].

Other important battery properties are more difficult to directly access through *ab initio* computations. Cyclability for instance tends to be difficult to predict directly as many, not always well understood, phenomena can be at the origin of the capacity fade during the cycling of the battery [32]. Some indications of possible poor cyclability can be obtained by DFT computations though. For instance, a large instability versus decomposition product of the metastable delithiated state(s) (*i.e.* a tendency to convert instead of intercalate) and/or large volume change during delithiation are often indications of a possible irreversibility.

HIGH-THROUGHPUT COMPUTATIONAL SCREENING

As first principles computations are capable of predicting properties of not-yet characterized materials, the idea of performing large scale high-throughput computational screening comes naturally. Performing thousands of computations on large databases of known or yet-to-be-made compounds offers to identify the materials combining the necessary properties for a given application. This method has been used recently in several fields from catalysis and thermo-electrics to transparent conductors and piezoelectric materials [33, 34, 35, 36, 37, 38, 39, 40]. It is worth mentioning that such a development was not only enabled by the increase in computational power and quality of *ab initio* code but also by strong efforts towards the automation of computations that used to require a large amount of human monitoring [41, 42, 29, 43].

In the battery field, the first high-throughput search for new battery materials was conducted in Professor Ceder's group at MIT and targeted cathode materials.This work screened more than 40,000 cathode materials on various
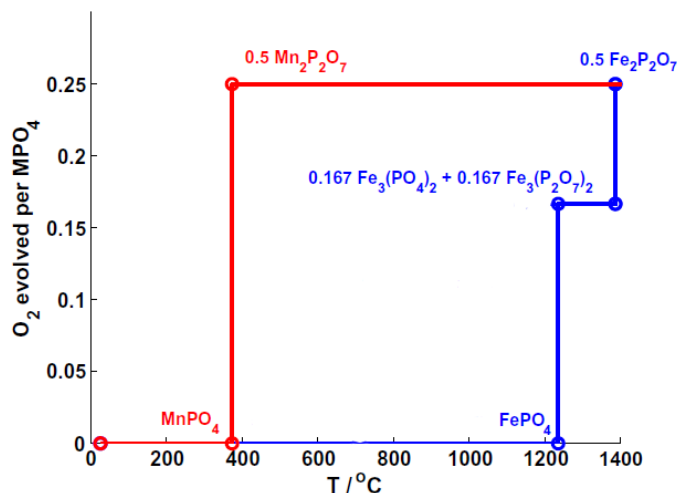
FIGURE 3. Computed oxygen released in MPO_4 in function of temperature for M=Fe and M=Mn. The MnPO$_4$ phase is not as thermally stable as FePO$_4$. Adapted from Ong *et al.* [18].

properties: capacity, stability (in the charged and discharged state), voltage and Li-ion diffusion. The project targeted known phases from the Inorganic Crystal Structure Database (ICSD) [44] but also previously unknown compounds using high-throughput compound prediction tools [45, 46, 47].

Discovery and Design of New Electrode Materials

The first outcome of a high-throughput computational screening project is to identify new cathode materials. One of the most interesting materials to emerge from our computational screening was monoclinic LiMnBO$_3$. This phase was previously known but had never been tested electrochemically. However, its polymorph LiMnBO$_3$ hexagonal phase had been characterized as a cathode material with very low capacity and poor performances. Our computational screening indicated that the monoclinic phase was of great interest with attractive voltage, capacity (due to the low weight of boron) and better Li-ion diffusion than the hexagonal phase. Follow-up experimental work indeed confirmed our computational finding with a capacity much larger than the hexagonal polymorph (see Fig. 4) [48]. Recently, the material performances have been further enhanced with a substantial capacity of 200 mAh/g achieved on an optimized material [49, 50]. The monoclinic manganese borate is an interesting example of a phase that was known but overlooked. The focus on the poor electrochemical performances of its hexagonal polymorph might have pushed the community to consider lithium manganese borates as inactive cathode materials. The strength of high-throughput screening lies here in its unbiased approach that can help preventing to miss an interesting compound.

Next to previously known phases such as LiMnBO$_3$, identified as a promising cathode, high-throughput computing can also lead to the discovery of novel compounds synthesized. For instance, we predicted an yet to be unreported Li$_9$V$_3$(P$_2$O$_7$)$_3$(PO$_4$)$_2$ to be a very promising cathode material [47]. Experimental follow-up confirmed this prediction and characterized the material electrochemically [51]. More unusual chemistries have also been computationally discovered. Carbonophosphate containing both phosphates and carbonates groups is a very rare chemistry that is not used for any application but only known as minerals. The computational screening approach identified a series of Li$_3$M(CO$_3$)(PO$_4$) compounds (with M = Fe, Mn, Ni, Co) to be interesting cathode materials [47]. The manganese compound was especially appealing by its potential to deliver two electrons per transition metal (Mn^{2+}/Mn^{3+} and Mn^{3+}/Mn^{4+} couples) in an adequate voltage window. Follow-up experiments synthesized the material for the first time and confirmed its electrochemical activity within the expected voltage range [52, 53, 54]. The sodium version was investigated afterwards and showed appealing electrode properties as well [55, 56, 57, 58].
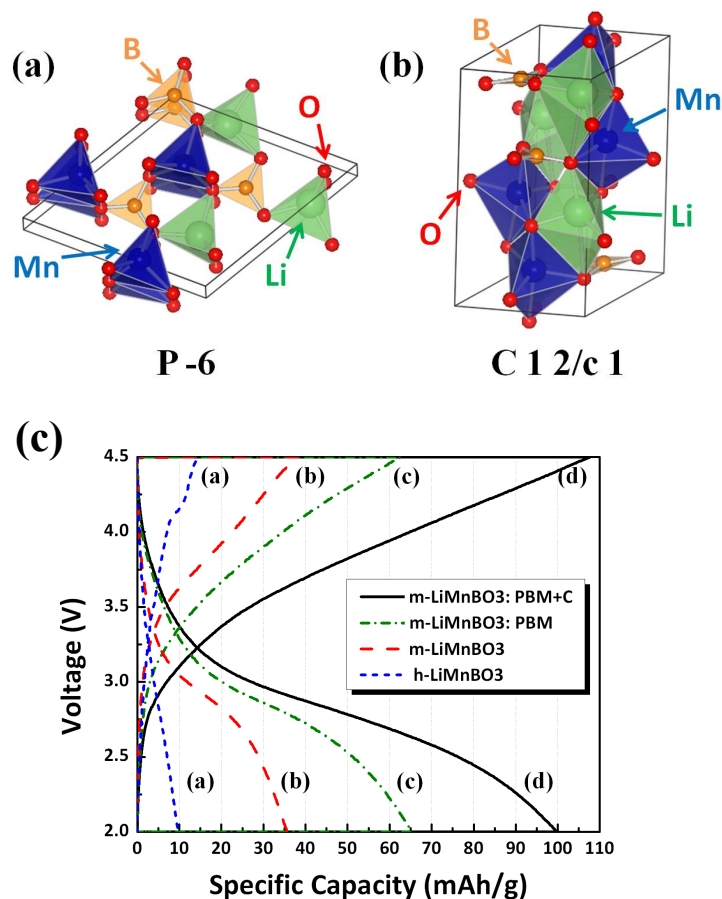
FIGURE 4. Hexagonal (a) and monoclinic (b) structures for LiMnBO$_3$. (c) Electrochemical results vs Li anode for the hexagonal (h) and monoclinic (m) phases under different preparation (with/without planetary ball-milling (PBM) and with/without carbon coating) [48].

Data Mining of High-Throughput Computed Data

The obvious use of computational screening is to identify the unique compounds with specific properties. However, high-throughput computing can offer more than this. By constructing large databases of computed properties, it is possible to search for trends and correlations within the data, performing what is now commonly called data mining.

We performed a series of data mining studies on the data generated by our high-throughput work. For instance, we focused on the very interesting tavorite structural framework to study how specific chemistries would affect essential properties such as stability, voltage and thermal stability [59]. This study lead to the proposed design of tavorite solid solutions that combine attractive voltages and high thermal stability for the charged state [38].

Tackling a larger chemical space than tavorites, we performed another data mining study targeting phosphate cathodes in general [47]. In this work, we studied over a thousand compounds in the Li-M-P-O chemical systems (where M is a redox active species) to mine what type of theoretical capacity, stability and voltage they could deliver. One of the important results of the study is to provide a voltage range in phosphate for each redox couple (see Fig. 5a). With this information, we can identify redox couples of interest and those that will lead to a too high or too low voltage. For instance, the couples Ni^{2+}/Ni^{3+} and Ni^{3+}/Ni^{4+} are very unlikely to be used with current liquid electrolytes because of their very high voltage (> 4.5 V). The study goes further and combine average voltage and best theoretical capacity as shown in Fig. 5b. If the target is to perform better than the typical phosphate-based cathode (LiFePO$_4$) in terms of specific energy, Fig. 5b shows that only a few redox couples can do so with one electron per transition metal and a voltage window that does not exceed 4.5 V: Fe^{2+}/Fe^{3+}, Mn^{2+}/Mn^{3+}, and Cu^{1+}/Cu^{2+}. While iron and
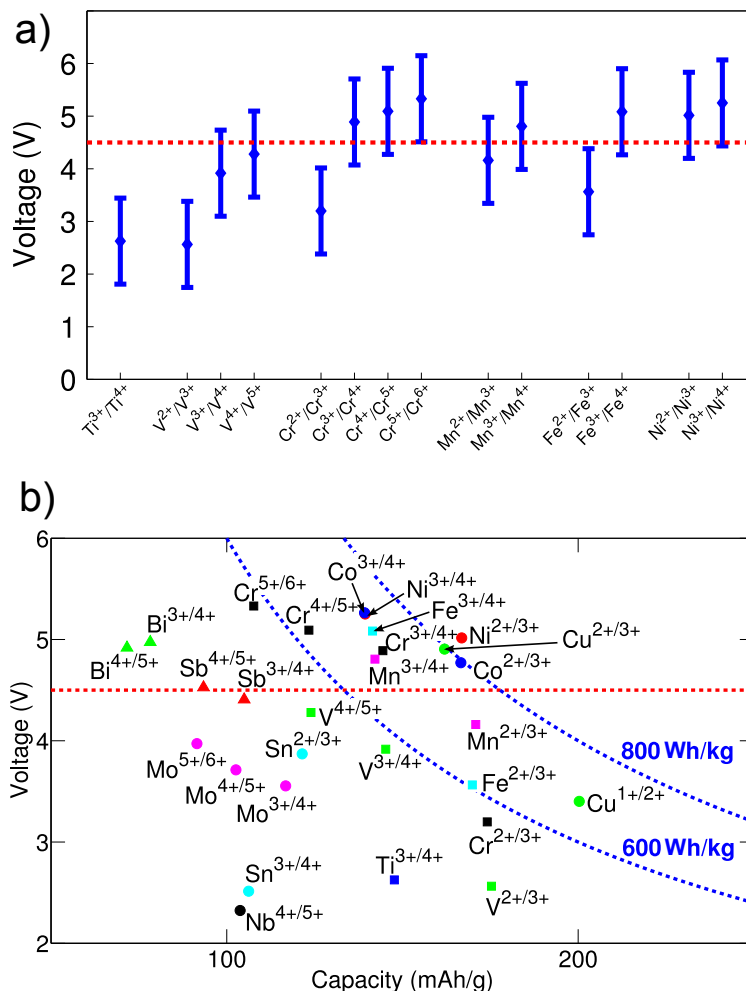
FIGURE 5. (a) Voltage ranges for a series of redox couples in phosphates. The blue bar indicates a voltage range due to structural effects. (b) Average voltage vs gravimetric capacity for all possible redox couples in phosphates. The blue dashed lines indicate lines of iso-specific energy and the red dashed line the limit of 4.5 V for electrolyte decomposition [47].

manganese have been extensively studied in phosphates, the data mining study motivated a study of copper-based cathodes that confirmed their attractive voltage (but potentially Cu migration issues) [60]. The real breakthrough in phosphate materials will come from the development of cathodes using more than one electron per transition metal. Figure 5b shows that only a few redox couples are again of interest here with voltages lower than the 4.5 V limit for liquid electrolytes: $V^{3+}/V^{4+}/V^{5+}$ or $Mo^{3+}/Mo^{4+}/Mo^{5+}/Mo^{6+}$. Despite its larger weight, molybdenum shows a very interesting multiple redox activity. This work has encouraged more experimental studies in the chemistry of molybdenum phosphates [61].

More recently, we used data mining on high-throughput computed data to study the relation between voltage and thermal stability of cathode materials in a large range of chemistries. A study from Huggins *et al.* in the 1980s pointed out that voltage and thermal stability of the charged state (indicated by the thermodynamical oxygen chemical potential of oxygen release or the temperature of oxygen release) are correlated [62]. High voltage cathodes tend to release oxygen more easily and are less safe. However, Huggins' study only presented results on conversion reactions and for a handful of compounds. Using our large database of thousands of cathode materials, we looked at a similar relationship between the computed insertion voltage and the computed temperature of oxygen release following the methodology developed by Ong *et al.* [18, 43]. Figure 6a plots the voltage versus decomposition temperature relationship. It confirms the correlation hinted by Huggins. However, there are differences depending on the chemistry
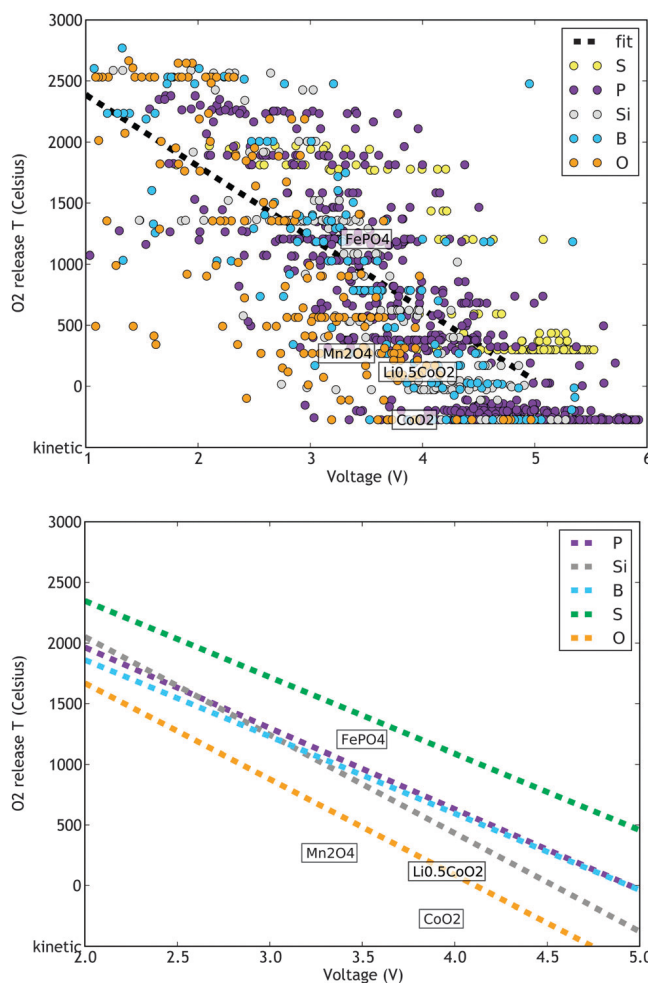
FIGURE 6. (a) Computed temperature of O_2 release vs voltage for a large database of cathode materials (b) Least-square linear fit of the data in (a) for each chemistries [43].

at play as indicated by Fig. 6b. Polyanionic cathodes (phosphates, silicates, borates) present a different behavior than oxides. For the same safety, they will provide higher voltages. This confirms the empirically observed safety advantage for polyanionic materials. However, our study also indicates that while polyanionic cathodes can offer a benefit in terms of thermal stability vs voltage, the presence of a polyanion group does not guarantee a high safety. Materials such as $LiCoPO_4$ for instance have indeed shown both experimentally and theoretically a strong tendency to easily release oxygen [63]. Moreover, the use of polyanions come with a price to pay in terms of gravimetric and volumetric capacity, especially for condensed polyanions (*e.g.*, pyrophosphates P_2O_7).

High-Throughput Computational Databases and the Materials Project

High-throughput computational studies generate large amounts of data. The highest scientific impact will be achieved not only by traditional scientific publication but also by a widespread diffusion of the generated data. Modern web and databases technologies offer to perform this painlessly and several high-throughput computational databases have emerged recently: The Materials Project [64, 65], AFLOWLib [66, 67] or the NOMAD database [68]. These databases cover a wide range of materials thermodynamical, electronic structure or mechanical properties. In terms of battery properties, the Materials Project database offers a specific web application providing computed materials properties (voltage profile and stability) for thousands of compounds [69].

PERSPECTIVE AND CONCLUSION

Since their first use in the end of the 1990s, first principles computations have become a standard tool in the study of materials for Li-ion batteries. We are clearly entering an exciting era where this computational tool will be more and more used to perform predictions and orient the experimental work. High-throughput evaluation of potential materials has already started for Li-ion batteries and led to very interesting studies using theory to guide experiments. High-throughput computing studies provide also very valuable data sets to perform data mining. While this short review focused on Li-ion batteries and especially inorganic cathodes, *ab initio* computational design is already extended to new emerging problems in energy storage including the move towards sodium-based [70, 71, 72, 73, 74, 75] and multi-valent batteries [76, 77] as well as solid-state electrolytes [26, 27, 28, 29, 30]. There is no doubt that these new fields will also strongly benefit from the power of first principles computational materials design.

REFERENCES

[1]   M. S. Whittingham, Chem. Rev. **104**, 4271–4302 (2004).
[2]   J. B. Goodenough and Y. Kim, Chem. Mater. **22**, 587–603 (2010).
[3]   B. L. Ellis, K. T. Lee, and L. F. Nazar, Chem. Mater. **22**, 691–714 (2010).
[4]   G. Jeong, Y. Kim, H. Kim, Y. Kim, and H. Sohn, Energy Environ. Sci. 1986–2002 (2011).
[5]   Y. S. Meng and M. E. Arroyo-de Dompablo, Energy & Environ. Sci. **2**, p. 589 (2009).
[6]   Y. S. Meng and M. E. Arroyo-de Dompablo, Acc. Chem. Res. **46**, 1171–1180 (2013).
[7]   G. Ceder, G. Hautier, A. Jain, and S. P. Ong, MRS Bull. **36**, 185–191 (2011).
[8]   M. D. Bhatt and C. O'Dwyer, Phys. Chem. Chem. Phys. **17**, 4799–4844 (2015).
[9]   R. A. Huggins, *Advanced Batteries: Materials Science Aspects* (Springer, 2008) p. 474.
[10]   J. Cabana, L. Monconduit, D. Larcher, and M. R. Palacín, Adv. Mater. **22**, E170–E192 (2010).
[11]   E. A. Carter, Science **321**, 800–803 (2008).
[12]   J. Hafner, C. Wolverton, and G. Ceder, MRS Bull. **31**, 659–668 (2006).
[13]   M. K. Aydinol, A. F. Kohan, G. Ceder, K. Cho, and J. Joannopoulos, Phys. Rev. B **56**, 1354–1365 (1997).
[14]   F. Zhou, M. Cococcioni, C. A. Marianetti, D. Morgan, and G. Ceder, Phys. Rev. B **70**, p. 235121 (2004).
[15]   J. Heyd, G. E. Scuseria, and M. Ernzerhof, J. Chem. Phys. **118**, p. 8207 (2003).
[16]   V. L. Chevrier, S. P. Ong, R. Armiento, M. K. Y. Chan, and G. Ceder, Phys. Rev. B **82**, p. 075122 (2010).
[17]   G. Ceder, Y. Chiang, D. R. Sadoway, M. K. Aydinol, Y. I. Jang, and B. Huang, Nature **392**, 694–696 (1998).
[18]   S. P. Ong, A. Jain, G. Hautier, B. Kang, and G. Ceder, Electrochem. commun. **12**, 427–430 (2010).
[19]   A. Van Der Ven, M. K. Aydinol, G. Ceder, G. Kresse, and J. Hafner, Phys. Rev. B **58**, 2975–2987 (1998).
[20]   J. Bhattacharya and A. Van Der Ven, Phys. Rev. B **81**, p. 104304 (2010).
[21]   K. Kang, D. Morgan, and G. Ceder, Phys. Rev. B **79**, p. 014305 (2009).
[22]   D. Morgan, A. Van Der Ven, and G. Ceder, Electrochem. Solid-State Lett. **7**, p. A30 (2004).
[23]   K. Kang, Y. S. Meng, J. Bréger, C. P. Grey, and G. Ceder, Science **311**, 977–980 (2006).
[24]   J. Lee, A. Urban, X. Li, D. Su, G. Hautier, and G. Ceder, Science **343**, 519–522 (2014).
[25]   A. Urban, J. Lee, and G. Ceder, Adv. Energy Mater. **4**, p. 1400478 (2014).
[26]   Z. Deng, B. Radhakrishnan, and S. P. Ong, Chem. Mater. **27**, 3749–3755 (2015).
[27]   L. J. Miara, S. P. Ong, Y. Mo, W. D. Richards, Y. Park, J.-M. Lee, H. S. Lee, and G. Ceder, Chem. Mater. **25**, 3048–3055 (2013).
[28]   L. J. Miara, W. D. Richards, Y. E. Wang, and G. Ceder, Chem. Mater. **27**, 4040–4047 (2015).
[29]   S. P. Ong, W. D. Richards, A. Jain, G. Hautier, M. Kocher, S. Cholia, D. Gunter, V. L. Chevrier, K. A. Persson, and G. Ceder, Comput. Mater. Sci. **68**, 314–319 (2013).
[30]   Y. Mo, S. P. Ong, and G. Ceder, Chem. Mater. **24**, 15–17 (2012).
[31]   T. Maxisch, F. Zhou, and G. Ceder, Phys. Rev. B **73**, p. 104301 (2006).
[32]   P. Arora, R. White, and M. Doyle, J. Electrochem. Soc. **145**, p. 3647 (1998).
[33]   J. Greeley, T. F. Jaramillo, J. Bonde, I. B. Chorkendorff, and J. K. Nørskov, Nat. Mater. **5**, 909–913 (2006).
[34]   G. K. H. Madsen, J. Am. Chem. Soc. **128**, 12140–12146 (2006).
[35]   S. Curtarolo, G. L. W. Hart, M. B. Nardelli, N. Mingo, S. Sanvito, and O. Levy, Nat. Mater. **12**, 191–201 (2013).
[36]   J. Carrete, W. Li, N. Mingo, S. Wang, and S. Curtarolo, Phys. Rev. X **4**, p. 011019 (2014).
[37]   S. Wang, Z. Wang, W. Setyawan, N. Mingo, and S. Curtarolo, Phys. Rev. X **1**, p. 021012 (2011).
[38]   G. Hautier, A. Jain, T. Mueller, C. Moore, S. P. Ong, and G. Ceder, Chem. Mater. **25**, 2064–2074 (2013).

[39] G. Hautier, A. Miglio, D. Waroquiers, G. Rignanese, and X. Gonze, Chem. Mater. **26**, 5447–5458 (2014).
[40] R. Armiento, B. Kozinsky, G. Hautier, M. Fornari, and G. Ceder, Phys. Rev. B **89**, p. 134103 (2014).
[41] W. Setyawan and S. Curtarolo, Comput. Mater. Sci. **49**, 299–312 (2010).
[42] A. Jain, G. Hautier, C. J. Moore, S. Ping Ong, C. C. Fischer, T. Mueller, K. A. Persson, and G. Ceder, Comput. Mater. Sci. **50**, 2295–2310 (2011).
[43] A. Jain, S. P. Ong, W. Chen, B. Medasani, X. Qu, M. Kocher, M. Brafman, G. Petretto, G.-M. Rignanese, G. Hautier, D. Gunter, and K. A. Persson, Concurr. Comput. Pract. Exp. **27**, 5037–5059 (2015).
[44] ICSD, Inorganic Crystal Structure Database, 2012.
[45] C. C. Fischer, K. J. Tibbetts, D. Morgan, and G. Ceder, Nat. Mater. **5**, 641–646 (2006).
[46] G. Hautier, C. C. Fischer, A. Jain, T. Mueller, and G. Ceder, Chem. Mater. **22**, 3762–3767 (2010).
[47] G. Hautier, A. Jain, S. P. Ong, B. Kang, C. Moore, R. Doe, and G. Ceder, Chem. Mater. **23**, 3945–3508 (2011).
[48] J. C. Kim, C. J. Moore, B. Kang, G. Hautier, A. Jain, and G. Ceder, J. Electrochem. Soc. **158**, p. A309 (2011).
[49] J. C. Kim, D.-H. Seo, and G. Ceder, Energy Environ. Sci. **8**, 1790–1798 (2015).
[50] J. C. Kim, D. Seo, H. Chen, and G. Ceder, Adv. Energy Mater. **5**, p. 1401916 (2015).
[51] A. Jain, G. Hautier, C. J. Moore, B. Kang, J. Lee, H. Chen, N. Twu, and G. Ceder, J. Electrochem. Soc. **159**, A622–A633 (2012).
[52] H. Chen, G. Hautier, and G. Ceder, J. Am. Chem. Soc. **134**, 19619–19627 (2012).
[53] H. Chen, G. Hautier, A. Jain, C. Moore, B. Kang, R. Doe, L. Wu, Y. Zhu, Y. Tang, and G. Ceder, Chem. Mater. **24**, 2009–2016 (2012).
[54] I. Matts, H. Chen, and G. Ceder, ECS Electrochem. Lett. **2**, A81–A83 (2013).
[55] H. Chen, Q. Hao, O. Zivkovic, G. Hautier, L. Du, Y. Tang, Y. Hu, X. Ma, C. P. Grey, and G. Ceder, Chem. Mater. **25**, 2777–2786 (2013).
[56] W. Huang, J. Zhou, B. Li, J. Ma, S. Tao, D. Xia, W. Chu, and Z. Wu, Sci. Rep. **4**, p. 4188 (2014).
[57] C. Wang, M. Sawicki, J. A. Kaduk, and L. L. Shaw, J. Electrochem. Soc. **162**, A1601–A1609 (2015).
[58] C. Wang, M. Sawicki, S. Emani, C. Liu, and L. L. Shaw, Electrochim. Acta **161**, 322–328 (2015).
[59] T. Mueller, G. Hautier, A. Jain, and G. Ceder, Chem. Mater. **23**, 3854–3862 (2011).
[60] K. Snyder, B. Raguž, W. Hoffbauer, R. Glaum, H. Ehrenberg, and M. Herklotz, Zeitschrift für Anorg. und Allg. Chemie **640**, 944–951 (2014).
[61] B. Wen, N. A. Chernova, R. Zhang, Q. Wang, F. Omenya, J. Fang, and M. S. Whittingham, Chem. Mater. **25**, 3513–3521 (2013).
[62] N. A. Godshall, I. D. Raistrick, and R. A. Huggins, J. Electrochem. Soc. **131**, p. 543 (1984).
[63] N. N. Bramnik, K. Nikolowski, D. M. Trots, and H. Ehrenberg, Electrochemical and Solid-State Letters **11**, A89–A93 (2008).
[64] A. Jain, S. P. Ong, G. Hautier, W. Chen, W. D. Richards, S. Dacek, S. Cholia, D. Gunter, D. Skinner, G. Ceder, and K. A. Persson, APL Mater. **1**, p. 011002 (2013).
[65] Materials Project, Http://www.materialsproject.org.
[66] S. Curtarolo, W. Setyawan, S. Wang, J. Xue, K. Yang, R. H. Taylor, L. J. Nelson, G. L. W. Hart, S. Sanvito, M. Buongiorno-Nardelli, N. Mingo, and O. Levy, Comput. Mater. Sci. **58**, 227–235 (2012).
[67] Aflowlib, Http://aflowlib.org/.
[68] Nomad, Http://nomad-repository.eu/cms/.
[69] Battery Materials Project Explorer, Http://www.materialsproject.org/#search/batteries.
[70] S. P. Ong, V. L. Chevrier, G. Hautier, A. Jain, C. Moore, S. Kim, X. Ma, and G. Ceder, Energy Environ. Sci. **4**, p. 3680 (2011).
[71] H. Kim, D. J. Kim, D. Seo, M. S. Yeom, K. Kang, D. K. Kim, and Y. Jung, Chem. Mater. **24**, 1205–1211 (2012).
[72] S. Kim, X. Ma, S. P. Ong, and G. Ceder, Phys. Chem. Chem. Phys. **14**, 15571–8 (2012).
[73] S. W. Kim, D. H. Seo, X. Ma, G. Ceder, and K. Kang, Adv. Energy Mater. **2**, 710–721 (2012).
[74] G. Rousse, M. E. Arroyo-de Dompablo, P. Senguttuvan, A. Ponrouch, J.-M. Tarascon, and M. R. Palacín, Chem. Mater. **25**, 4946–4956 (2013).
[75] Y. Mo, S. P. Ong, and G. Ceder, Chem. Mater. **26**, 5208–5214 (2014).
[76] M. Liu, Z. Rong, R. Malik, P. Canepa, A. Jain, G. Ceder, and K. A. Persson, Energy Environ. Sci. **8**, 964–974 (2015).
[77] G. Sai Gautam, P. Canepa, A. Abdellahi, A. Urban, R. Malik, and G. Ceder, Chem. Mater. **27**, 3733–3742 (2015).